Novel Aldosterone Synthase Inhibitors with Extended Carbocyclic Skeleton by a Combined Ligand-Based and Structure-Based Drug Design Approach

Simon Lucas,[†] Ralf Heim,[†] Matthias Negri,[†] Iris Antes,[‡] Christina Ries,[†] Katarzyna E. Schewe,[†] Alessandra Bisi,[§] Silvia Gobbi,[§] and Rolf W. Hartmann*[,†]

Pharmaceutical and Medicinal Chemistry, Saarland University, P.O. Box 151150, D-66041 Saarbrücken, Germany, Max Planck Institute for Informatics, Stuhlsatzenhausweg 85, D-66123 Saarbrücken, Germany, Department of Pharmaceutical Sciences, University of Bologna, Via Belmeloro 6, I-40126 Bologna, Italy

Received June 5, 2008

Pharmacophore modeling of a series of aldosterone synthase (CYP11B2) inhibitors triggered the design of compounds **11** and **12** by extending a previously established naphthalene molecular scaffold (e.g., present in molecules **1** and **2**) via introduction of a phenyl or benzyl residue in 3-position. These additional aromatic moieties have been hypothesized to fit into the newly identified hydrophobic pharmacophore feature HY3. Subsequent docking studies in our refined CYP11B2 protein model have been performed prior to synthesis to estimate the inhibitory properties of the proposed molecules. While phenyl-substituted compound **11** (IC_{50} > 500 nM) did not dock under the given pharmacophore constraint (i.e., the Fe(heme)−N(ligand) interaction), benzyl-substituted compound **12** (IC_{50} = 154 nM) was found to exploit a previously unexplored subpocket of the inhibitor binding site. By structural optimization based on the pharmacophore hypothesis, 25 novel compounds were synthesized, among them highly potent CYP11B2 inhibitors (e.g., **17**, IC_{50} = 2.7 nM) with pronounced selectivity toward the most important steroidogenic and hepatic CYP enzymes.

Introduction

Aldosterone synthase (CYP11B2[a]), a mitochondrial cytochrome P450 enzyme that is localized mainly in the adrenal cortex, is the key enzyme of mineralocorticoid biosynthesis. It catalyzes the terminal three oxidation steps in the biogenesis of aldosterone in humans.[1] This hormone is the most important circulating mineralocorticoid and plays a crucial role in the electrolyte and fluid homeostasis mainly by binding to epithelial mineralocorticoid receptors (MR), promoting sodium reabsorption and potassium secretion. Because the sodium movement is followed by water via osmosis, aldosterone is a key regulator of blood volume and blood pressure. Abnormally increased plasma levels of aldosterone have been diagnosed in different cardiovascular diseases such as elevated blood pressure, congestive heart failure, and myocardial fibrosis.[2] Inhibitors of the angiotensin-converting enzyme (ACE), which are in use for the treatment of hypertension and congestive heart failure, can initially induce a down-regulation of circulating aldosterone. However, increased levels of aldosterone are frequently observed after several months of therapy.[3] This phenomenon termed "aldosterone escape" is a limiting factor of ACE inhibitors and shows that novel therapeutic concepts combating the effects of elevated aldosterone levels are needed. Two recent clinical studies (RALES and EPHESUS) demonstrated that treatment with mineralocorticoid receptor antagonists in addition to the standard therapy resulted in a decrease of mortality in patients with chronic congestive heart failure and in patients after myocardial infarction, respectively.[4,5] The use of spironolactone, however, is accompanied by severe progestational and antiandrogenic side effects due to its affinity to other steroid receptors. Moreover, the elevated plasma aldosterone concentrations are left unaffected on a pathological level, which raises several issues. First, the elevated aldosterone plasma levels do not induce a homologous down-regulation but an up-regulation of the aldosterone receptor.[6] This fact complicates a long-term therapy as MR antagonists are likely to become ineffective. Furthermore, the high concentrations promote nongenomic actions of aldosterone, which are in general not blocked by receptor antagonists.[7] Pathological aldosterone concentrations have been identified to induce a negative inotropic effect in human trabeculae and to potentiate the vasoconstrictor effect of angiotensin II in coronary arteries in rapid, nongenomic manner.[8] Thus, aldosterone is intrinsically capable to further deteriorate heart function by acting nongenomically.

A novel therapeutic strategy with potential to overcome the drawbacks of MR antagonists is the blockade of aldosterone formation, preferably by inhibiting CYP11B2, the key enzyme of its biosynthesis. Aldosterone synthase has been proposed as a potential pharmacological target by our group as early as 1994,[9] followed soon thereafter by the hypothesis that inhibitors of CYP11B2 could serve as drugs for the treatment of hyperaldosteronism, congestive heart failure, and myocardial fibrosis.[10,11] Consequent structural optimization of a hit discovered by a compound library screening led to a series of nonsteroidal aldosterone synthase inhibitors with high selectivity toward other cytochrome P450 enzymes.[12−15]

In the present study, we describe the design and synthesis of a series of 3-benzyl-substituted pyridylnaphthalenes and structurally related compounds (Chart 1) by a combined ligand-based and structure-based drug design approach as well as the determination of their biological activity regarding human CYP11B2 for potency. Selectivity is a prerequisite for a CYP11B2 inhibitor, especially with regard to other cytochrome

* To whom correspondence should be addressed: Phone: +49 681 302 2424. Fax: +49 681 302 4386. E-mail: rwh@mx.unisaarland.de.
[†] Pharmaceutical and Medicinal Chemistry, Saarland University.
[‡] Max Planck Institute for Informatics.
[§] Department of Pharmaceutical Sciences, University of Bologna.

[a] Abbreviations: ACE, angiotensin-converting enzyme; AUC, area under the curve; CYP, cytochrome P450; CYP11B1, 11β-hydroxylase; CYP11B2, aldosterone synthase; CYP17, 17α-hydroxylase-17,20-lyase; CYP19, aromatase; EPHESUS, eplerenone postacute myocardial infarction heart failure efficacy and survival study; MR, mineralocorticoid receptor; RALES, randomized aldactone evaluation study; SAR, structure−activity relationship; TEMPO, 2,2,6,6-tetramethylpiperidin-1-oxyl.

10.1021/jm800683c CCC: $40.75
Published on Web 09/03/2008

Chart 1. Title Compounds

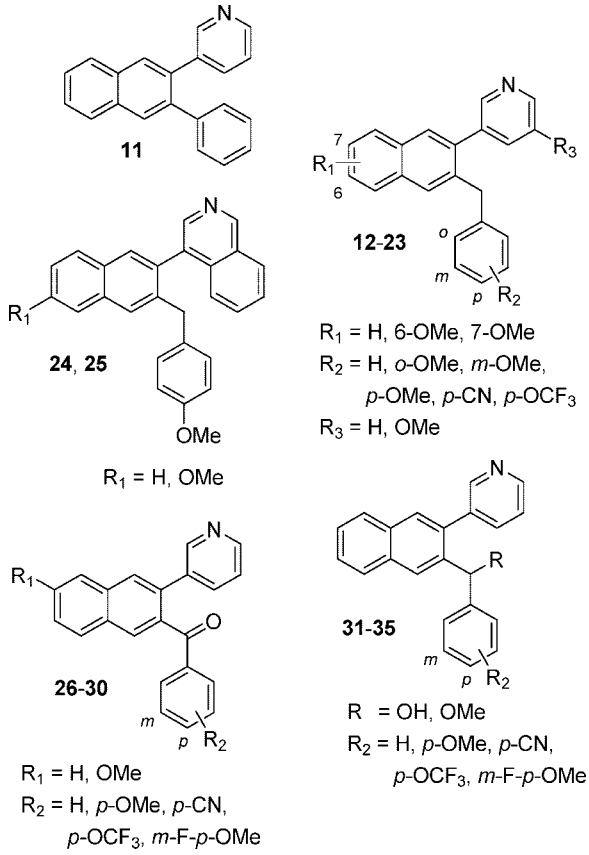

P450 enzymes, as they are likely to interact with other CYP enzymes in a similar way (e.g., by complexation of the heme iron). Taking into consideration that the key enzyme of glucocorticoid biosynthesis, 11β-hydroxylase (CYP11B1), and CYP11B2 have a sequence homology of approximately 93%,[16] the selectivity issue becomes especially critical for the design of CYP11B2 inhibitors. On that account, all compounds were tested for their inhibitory potency toward CYP11B1 to determine their selectivity. A set of compounds was additionally tested for inhibitory activity toward the steroidogenic enzymes CYP17 (17α-hydroxylase-C17,20-lyase) and CYP19 (aromatase) as well as selected hepatic drug-metabolizing CYP enzymes (CYP1A2, CYP2B6, CYP2C9, CYP2C19, CYP2D6, and CYP3A4).

Results

Inhibitor Design Concept. In our search for new lead compounds as CYP11B2 inhibitors that are structurally different from the previously discovered pyridylnaphthalenes such as **1** and **2**,[14] we identified imidazolylmethylene-substituted flavones (e.g., **3**−**10**) to be aldosterone synthase inhibitors with moderate to high inhibitory potency by compound library screening (Table 1). These compounds that originally have been described as aromatase inhibitors[17] display CYP11B2 inhibition in a range of 73−94% at a concentration of 500 nM, with methoxy-functionalized **6** being most active (IC_{50} = 11 nM), albeit without showing selectivity toward the highly homologous CYP11B1 (see Supporting Information for selectivity data). Recently, a pharmacophore model for aldosterone synthase inhibitors was built by superimposition of a series of heteroaryl-substituted methyleneindanes[12,13] and naphthalenes[14,15] synthesized in our laboratory and subsequently validated by pyridine-substituted acenaphthenes as hybrid structures that fit into the four identified pharmacophoric points (i.e., a heterocyclic

Table 1. Inhibition of Human Adrenal CYP11B2 In Vitro (Compounds **1**−**10**)

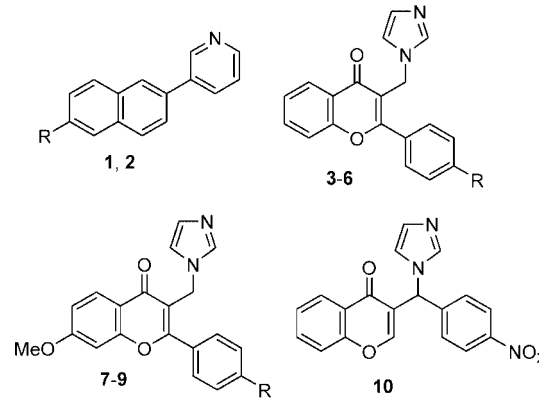

compd	R	% inhibition[a] CYP11B2[b] [IC_{50} (nM)[c]]
1	H	92 [28]
2	OMe	91 [6.2]
3	H	88 [28]
4	NO_2	81 [95]
5	Br	90 [25]
6	OMe	94 [11]
7	H	86 [124]
8	Br	80 [n.d.]
9	NO_2	73 [n.d.]
10		77 [187]

[a] Mean value of at least two experiments, standard deviation usually less than 10%; inhibitor concentration, 500 nM. [b] Hamster fibroblasts expressing human CYP11B2; substrate deoxycorticosterone, 100 nM. [c] Mean value of at least four experiments, standard deviation usually less than 25%, n.d. = not determined; fadrozole, IC_{50} = 1 nM.

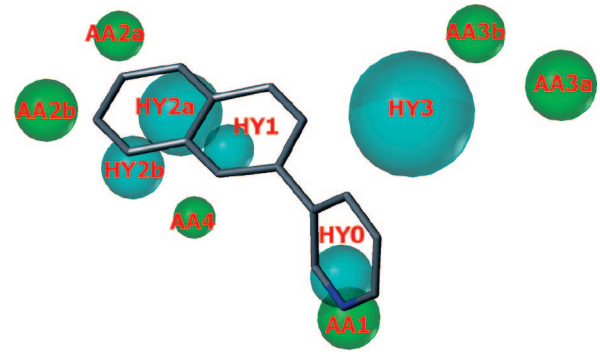

Figure 1. Compound **1** mapped to the pharmacophore model. The newly identified hydrophobic feature HY3 as well as the acceptor atom features AA3a and AA3b are not exploited by inhibitors with a naphthalene molecular scaffold. Pharmacophoric features are color-coded: cyan for hydrophobic regions (HY0−HY3) and green for acceptor atom features (AA1−AA4).

nitrogen and three ring centroids).[18] The most potent compounds of the latter substance classes together with the most potent flavone type inhibitors were used as a training set for the generation of an extended pharmacophore model by applying the GALAHAD[19] pharmacophore generation module of SYBYL molecular modeling software. In the top ranked pharmacophore model, best in three of the most indicative ranking criteria of this software (Pareto ranking,[20] Specificity, and Mol-query), the earlier pharmacophoric points[18] were confirmed, namely the hydrophobic features HY0, HY1, HY2a, and HY2b as well as the acceptor atom features AA1, AA2a, and AA2b (Figure 1). A novel and voluminous hydrophobic area HY3 was identified next to HY1, along with the acceptor atom features AA3a and AA3b (see Supporting Information for exact pharmacophore

Chart 2. Proposed Lead Structures **11** and **12**

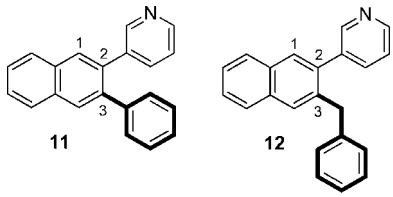

geometric properties) as well as an additional acceptor atom feature AA4. Rationalizing the given information, the two sample compounds **11** and **12** (Chart 2) were designed by modifying our previously reported naphthalene derivatives **1** and **2** to exploit the newly discovered pharmacophoric feature HY3. As suggested by the model and visualized in Figure 1, introduction of a hydrophobic substituent in 3-position of the naphthalene skeleton should be favorable to exploit the voluminous hydrophobic feature HY3 of the pharmacophore. The phenyl residue directly bound to the naphthalene core in compound **11** creates a conformationally constrained structure in which both rotational degrees of freedom of the two aryl−aryl bonds are limited because they are located *ortho* to each other. The benzyl motive in compound **12** leads to an increased flexibility of the spatial property distribution by rotation around the two benzylic carbon−carbon bonds. Furthermore, the aromatic ring moves apart from the naphthalene core by one methylene unit.

To elucidate the role of conformational flexibility and the exact position of the aryl moiety for optimal inhibitor binding, docking studies were performed. For this purpose, we used the CYP11B2 protein model that has been built[12] and subsequently validated[13−15] by our group as well as the same docking calculations that have been performed in these studies. Previous investigations have identified the binding affinity to the target enzyme to be highly dependent on the geometry of the coordinative bond between the heme iron and the heterocyclic nitrogen. An angle of the Fe−N straight line with the porphyrine plane close to 90° (i.e., the heterocyclic nitrogen lone pair arranges perpendicular to the heme group) provides an optimal orbital overlap and corresponds with high inhibitory potency.[14,15] The analysis of the docking mode of compound **3** led to the identification of a new subpocket that interacts with the aryl moiety (Figure 2a). This subpocket was not considered as potential binding site during our previous design efforts due to the fact that the formerly investigated compounds such as **2** did not occupy this binding site (Figure 2b). The above considerations led to the design of compounds **11** and **12**. Both compounds combine the pyridylnaphthalene skeleton of compound **1** with an additional aryl motive, which should be able to interact with the newly identified subpocket. However, compound **11** proved to be too rigid to fit into the binding site and could thus not be docked successfully into the binding pocket under the given pharmacophore constraint, that is the Fe(heme)−N(ligand) interaction. A directed heme-Fe−N interaction was defined perpendicular to the heme plane. This pharmacophore constraint was applied to ensure the right binding mode of the inhibitors with the heme cofactor. The constraint requires the existence of an inhibitor nitrogen atom on the surface of an interaction cone with a 20° radius, which has its origin at the Fe atom and points perpendicular to the heme plane (with a length of 2.2 Å). Obviously, the conformationally restricted phenyl moiety of compound **11** undergoes repulsive interaction with amino acids of the binding pocket or with the heme cofactor under the above-mentioned constraint (i.e., when the pyridine moiety forms a coordinative bond to the heme iron), thus preventing that the molecule successfully docks into the CYP11B2 protein model. Contrariwise, the 3-benzyl substituted analog **12** is more flexible due to an additional methylene spacer between the two ring systems and thus fitted adequately into the binding site (Figure 2c). From these docking results, we concluded that the methylene group

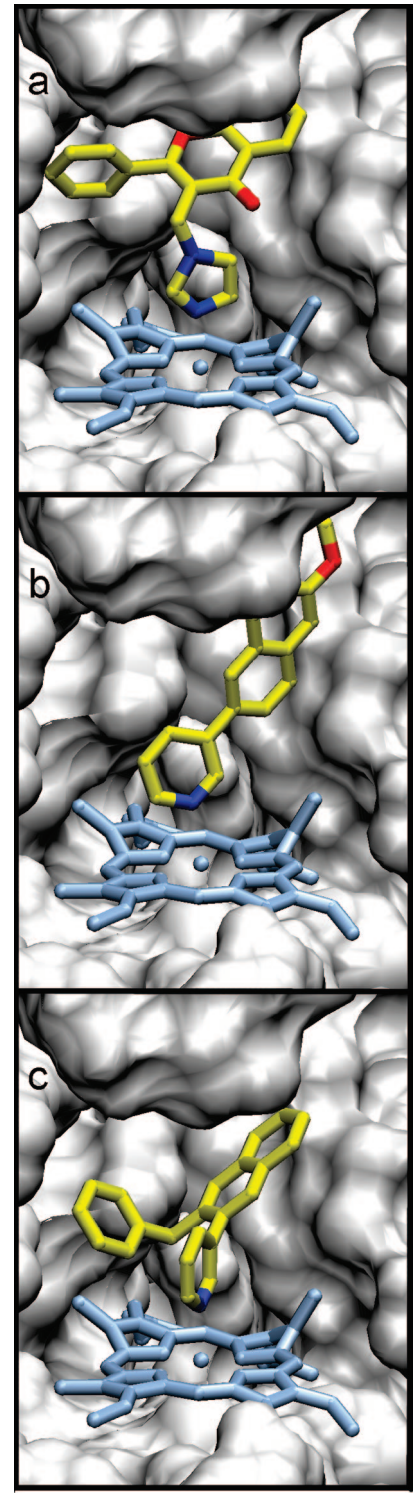

Figure 2. Structure of the CYP11B2−inhibitor complexes of **3** (a), **2** (b), and **12** (c). Surface of the binding pocket (gray) surrounding the inhibitor and the heme cofactor (light blue). The inhibitors are presented in yellow; nitrogen atoms are colored in blue, and oxygen atoms are in red. Unlike **2**, the inhibitors **3** and **12** exploit an additional subpocket of the inhibitor binding site.

Scheme 1[a]

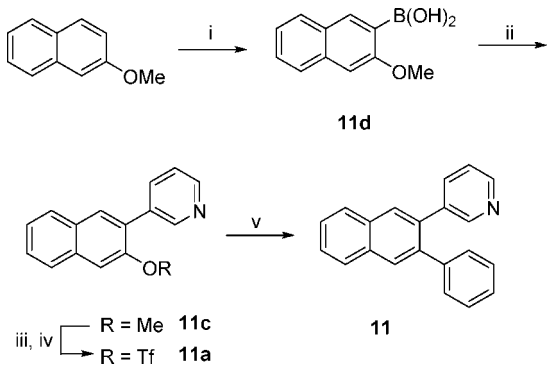

[a] Reagents and conditions: (i) *n*BuLi, $B(OMe)_3$, THF, −78 °C, then HCl/water; (ii) 3-bromopyridine, $Pd(PPh_3)_4$, toluene/ethanol, aq Na_2CO_3, reflux; (iii) conc. HBr, reflux; (iv) Tf_2NPh, K_2CO_2, THF, μw, 120 °C; (v) phenylboronic acid, $Pd(PPh_3)_4$, aq $NaHCO_3$, DMF, μw, 150 °C.

of the potential inhibitor should provide the flexibility necessary to adapt to the binding site geometry.

Chemistry. The phenyl-substituted pyridylnaphthalene **11** was obtained as shown in Scheme 1 by two subsequent Suzuki coupling[21] steps, whereof the first proceeded between 3-bromopyridine and 3-methoxy-2-naphthaleneboronic acid **11d**. The boronic acid **11d** was accessible by *ortho*-lithiation of 2-methoxynaphthalene and in situ addition of trimethylborate as described previously.[22] After demethylation of **11c** by refluxing in concentrated hydrobromic acid, the intermediate naphthol was transferred into the triflate **11a** by a microwave-enhanced method described by Bengtson et al.[23] A second Suzuki coupling using controlled microwave heating afforded compound **11**.[24]

The benzyl-substituted derivatives **12**−**16**, **19**, and **21**−**25** were synthesized by the route shown in Scheme 2. Starting from a 3-hydroxy-2-naphthoic acid, few functional group modifications led to the carbaldehydes **12e**−**14e**. These transformations were performed by a four-step sequence starting with an esterification[25] and subsequent introduction of a protection group to the naphthalene hydroxy group of **12h** and **13h** (i.e., methyl in **12g** or benzyl in **13g** and **14g**).[26] Lithium borohydride reduction[27] followed by TEMPO oxidation[28] (of primary alcohol **12f**) or Parik−Doehring oxidation[29] (of **13f** and **14f**) afforded the corresponding carbaldehydes **12e**−**14e**. Grignard reaction with various substituted phenylmagnesium halogenides afforded the phenyl−naphthylalcohols **12d**−**16d** and **19d**. Hydrogenolytic removal of the hydroxy group was accomplished by treatment with $NaBH_4$ and $AlCl_3$ in refluxing THF.[30] After deprotection using BBr_3 (for demethylation of **12c**) or ammonium formate under Pd-catalysis[31] (for debenzylation of **13c**−**16c** and **19c**) and subsequent triflate formation,[23] the heterocycle was introduced by microwave-enhanced Suzuki coupling,[24] giving rise to the benzyl-substituted pyridylnaphthalenes **12**−**16**, **19**, and **21**−**25**.

Alternatively, the benzyl-substituted pyridylnaphthalenes **17**, **18**, and **20** were obtained by the route shown in Scheme 3. Applying the presented transformations afforded the benzoyl-substituted derivatives **26**−**30** and the corresponding hydroxymethylene analogues **31**−**34** as reaction intermediates. The sequence toward the 3-benzoyl-substituted 2-naphthols **26b**−**30b** was reported previously by Li et al. and starts with an *ortho*-lithiation of 2-methoxy- or 2,7-dimethoxynaphthalene, followed by in situ addition of a Weinreb amide. Regioselective demethylation of the obtained methanones **26c**−**30c** at the naphthalene-position *ortho* to the benzoyl residue was accomplished by treatment with BCl_3/nBu_4NI at −78 °C.[32] After triflate formation, a 3-pyridyl residue was introduced by Suzuki coupling to afford compounds **26**−**30**. The corresponding alcohols **20a** and **31**−**34** were obtained by sodium borohydride reduction. The methyl ether **35** was synthesized by treating **31** with methyl iodide and NaH in THF. The benzyl-substituted pyridylnaphthalenes **17**, **18**, and **20** were obtained by in situ iodotrimethylsilane mediated reduction.[33,34] However, reduction by this method did not succeed in the case of **32** nor by other commonly used hydrogenolysis protocols.[30,35]

Biological Results

Inhibition of Human Adrenal Corticoid Producing CYP11B2 and CYP11B1 In Vitro (Table 2). The inhibitory activities of the compounds were determined in V79 MZh cells expressing either human CYP11B2 or CYP11B1.[10,36] The V79 MZh cells were incubated with [^{14}C]-deoxycorticosterone as substrate and the inhibitor in different concentrations. The product formation was monitored by HPTLC using a phosphoimager. Fadrozole, an aromatase (CYP19) inhibitor with proven ability to reduce corticoid formation in vitro[37] and in vivo,[38] was used as a reference (CYP11B2, IC_{50} = 1 nM; CYP11B1, IC_{50} = 10 nM).

Compound **11** with a phenyl residue directly bound to the naphthalene core shows no significant activity at the target enzyme with only 8% inhibition at an inhibitor concentration of 500 nM (Table 2). Insertion of a methylene linker into the biaryl bond results in an increased inhibitory potency at CYP11B2 in compound **12** (IC_{50} = 154 nM). Introduction of a methoxy residue in *ortho*- or *meta*-position of the benzylic moiety as accomplished in compounds **14** and **15** results in a significantly decreased inhibitory potency, whereas the same substituent in *para*-position gives rise to the highly potent CYP11B2 inhibitor **16** (IC_{50} = 7.8 nM) with pronounced selectivity toward CYP11B1 (IC_{50} = 2804). The cyano and trifluoromethoxy-substituted analogues **17** and **18** are also highly potent as well and about 700-fold and 900-fold more selective for CYP11B2. Derivatization of the naphthalene core by a methoxy group is readily tolerated in 6-position as accomplished in compounds **13**, **19**, **22**, **23**, and **25**. The inhibitory profile of the 6-methoxy derivatives regarding the two CYP11B isoforms is comparable to the corresponding hydrogen analogues with a slightly increased selectivity factor in most cases. On the other hand, introduction of methoxy in 7-position results in a decrease of the inhibition to less than 40% at an inhibitor concentration of 500 nM (**20** and **30**). Modification of the pyridine moiety, which has recently been shown to increase the activity and selectivity of naphthalene type CYP11B2 inhibitors,[39] affords compounds **21**−**25** with IC_{50} values in the range of 3−24 nM. Replacing the methylene linker by a carbonyl group as accomplished in compounds **26**−**29** results in a slightly reduced inhibitory potency (IC_{50} = 16−118 nM), albeit the high CYP11B1 selectivity is retained (factor 200−500). Introducing hydroxymethylene (**31**−**34**) or methoxymethylene (**35**) as linker between the aryls leads to a significant loss of inhibitory activity to approximately 60% at an inhibitor concentration of 500 nM in the case of compounds **31**−**34** and to an almost complete loss in the case of compound **35**.

Inhibition of Steroidogenic and Hepatic CYP Enzymes (Tables 3 and 4). A set of 12 compounds was investigated for inhibition of the steroidogenic enzymes CYP17 and CYP19 (Table 3). The inhibition of CYP17 was investigated using the 50000*g* sediment of the *Escherichia coli* homogenate recombinantly expressing human CYP17 and progesterone (25 μM) as substrate.[40] The inhibition values were measured at an

Scheme 2[a]

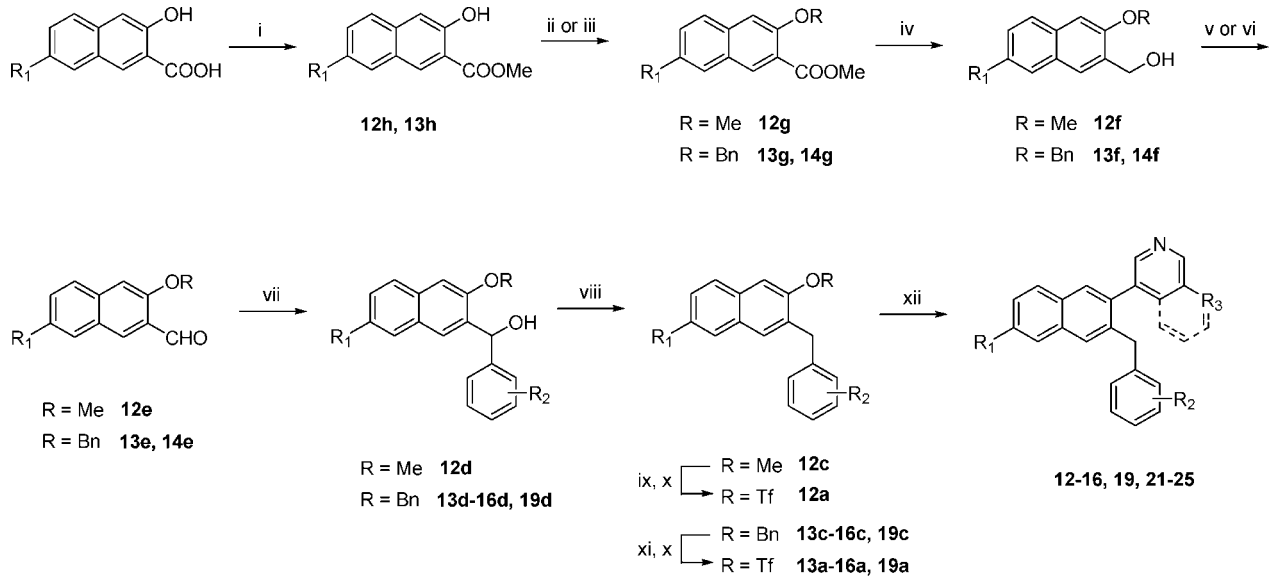

[a] Reagents and conditions: (i) methanol, H_2SO_4, reflux; (ii) MeI, K_2CO_3, 18-crown-6, acetone, reflux (for R = Me); (iii) BnBr, K_2CO_3, 18-crown-6, acetone, reflux (for R = Bn); (iv) $LiBH_4$, THF/toluene, reflux; (v) NCS, TEMPO, nBu$_4$NCl, aq Na_2CO_3/$NaHCO_3$, CH_2Cl_2; rt (for R = Me); (vi) SO_3·py, NEt_3, DMSO, rt (for R = Bn); (vii) ArMgX, THF, 0 °C, then aq NH_4Cl; (viii) $NaBH_4$, $AlCl_3$, THF, reflux; (ix) BBr_3, CH_2Cl_2, −20 °C; (x) Tf_2NPh, K_2CO_2, THF, μw, 120 °C; (xi) ammonium formate, Pd/C, THF/methanol, reflux; (xii) heteroarylboronic acid, $Pd(PPh_3)_4$, aq $NaHCO_3$, DMF, μw, 150 °C.

Scheme 3[a]

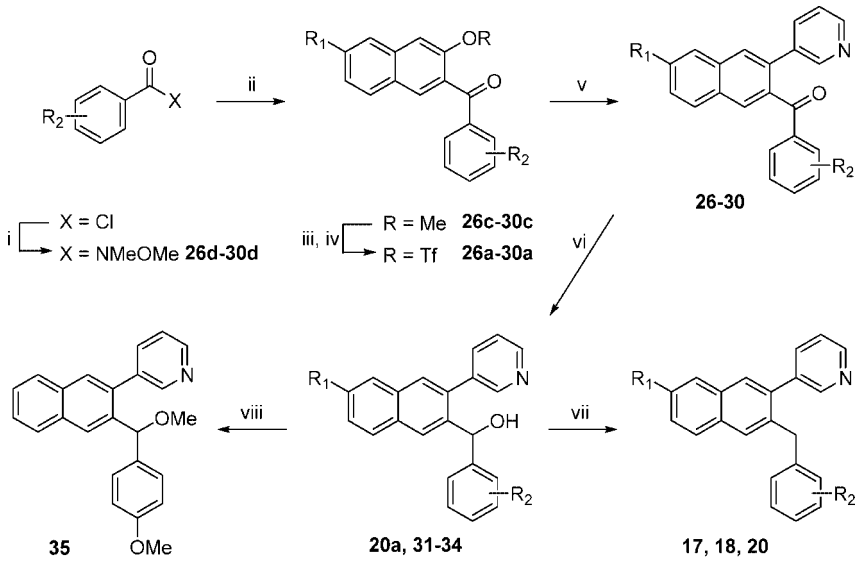

[a] Reagents and conditions: (i) *N*,*O*-dimethylhydroxylamine hydrochloride, NEt_3, CH_2Cl_2, rt; (ii) nBuLi, 2-methoxynaphthalene (for R_1 = H) or 2,7-dimethoxynaphthalene (for R_1 = OMe), TMEDA, THF, −78 °C, then HCl/water; (iii) BCl_3, nBu$_4$NI, CH_2Cl_2, −78 °C to rt; (iv) Tf_2O, pyridine, CH_2Cl_2, 0 °C; (v) pyridineboronic acid, $Pd(PPh_3)_4$, aq Na_2CO_3, toluene/ethanol, reflux; (vi) $NaBH_4$, methanol, 0 °C; (vii) Me_3SiCl, NaI, CH_3CN, 55 °C; (viii) MeI, NaH, THF, rt.

inhibitor concentration of 2 μM. In general, the compounds show no or only little inhibition of less than 25%. As an exception, compound **22** exhibits 51% inhibition, which is in the range of the reference ketoconazole (IC_{50} = 2780 nM). The inhibition of CYP19 at an inhibitor concentration of 500 nM was determined in vitro with human placental microsomes and [1β-^{3}H]androstenedione as substrate as described by Thompson and Siiteri[41] using our modification.[42] Most of the compounds display only a moderate aromatase inhibition of less than 40% whereof four compounds do not inhibit CYP19 at all (**21**, **24**, **25**, and **28**). The *para*-cyano-substituted derivative **17** shows a pronounced activity (60%) and introduction of methoxy in 6-position of the naphthalene core as accomplished in compounds **19**, **22**, and **23** results likewise in a remarkably increased inhibition. Most notably, compound **19** is a highly potent CYP19 inhibitor exhibiting an IC_{50} value of 38 nM, thus being almost as active as the reference fadrozole (IC_{50} = 30 nM).

A selectivity profile relating to inhibition of crucial hepatic CYP enzymes (CYP1A2, CYP2B6, CYP2C9, CYP2C19, CYP2D6, and CYP3A4) was determined for compounds **16**, **17**, **19**, and **28** by use of recombinantly expressed enzymes from baculovirus-infected insect microsomes. Table 4 shows the inhibition at a concentration of 10 and 1 μM. It becomes apparent that some enzymes are affected only to a minor degree by all compounds including CYB2B6 and CYP2D6. On the other hand, CYP2C9 is strongly inhibited in most cases. The benzoyl derivative **28** with less than 40% inhibition at 1 μM concentration at all CYP enzymes is the most selective

Table 2. Inhibition of Human Adrenal CYP11B2 and CYP11B1 In Vitro (Compounds **11**−**35**)

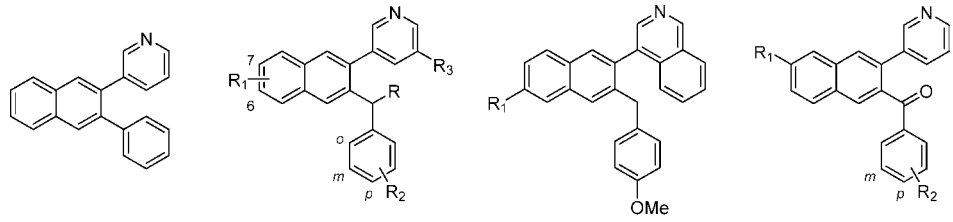

11 **12-23, 31-35** **24, 25** **26-30**

compd	R_1	R_2	R_3	R	% inhibition[a] V79 11B2[c] hCYP11B2	IC_{50} value[b] (nM) V79 11B2[c] hCYP11B2	V79 11B1[d] hCYP11B1	selectivity factor[e]
11					8	n.d.	n.d.	n.d.
12	H	H	H	H	76	154	953	6
13	6-OMe	H	H	H	85	53	640	12
14	H	*o*-OMe	H	H	24	n.d.	n.d.	n.d.
15	H	*m*-OMe	H	H	62	n.d.	n.d.	n.d.
16	H	*p*-OMe	H	H	89	7.8	2804	359
17	H	*p*-CN	H	H	93	2.7	1956	724
18	H	*p*-OCF_3	H	H	95	3.9	3559	913
19	6-OMe	*p*-OMe	H	H	95	11	4329	394
20	7-OMe	*p*-OMe	H	H	35	n.d.	n.d.	n.d.
21	H	*p*-OMe	OMe	H	93	7.7	1811	235
22	6-OMe	*p*-OMe	OMe	H	96	7.6	2452	322
23	6-OMe	H	OMe	H	90	24	2936	122
24	H				98	3.0	785	262
25	OMe				94	5.0	735	147
26	H	*p*-OMe	H		79	119	24003	202
27	H	*m*-F-*p*-OMe	H		78	65	19816	305
28	H	*p*-CN	H		88	30	9639	321
29	H	*p*-OCF_3	H		91	28	11307	404
30	OMe	*p*-OMe	H		25	n.d.	n.d.	n.d.
31	H	*p*-OMe	H	OH	57	n.d.	n.d.	n.d.
32	H	*m*-F-*p*-OMe	H	OH	51	n.d.	n.d.	n.d.
33	H	*p*-CN	H	OH	59	n.d.	n.d.	n.d.
34	H	*p*-OCF_3	H	OH	63	n.d.	n.d.	n.d.
35	H	*p*-OMe	H	OMe	23	n.d.	n.d.	n.d.
fadrozole						1	10	10

[a] Mean value of at least two experiments, standard deviation usually less than 10%; inhibitor concentration, 500 nM. [b] Mean value of at least four experiments, standard deviation usually less than 25%, n.d. = not determined. [c] Hamster fibroblasts expressing human CYP11B2; substrate deoxycorticosterone, 100 nM. [d] Hamster fibroblasts expressing human CYP11B1; substrate deoxycorticosterone, 100 nM. [e] IC_{50} CYP11B1/IC_{50} CYP11B2, n.d. = not determined.

Table 3. Inhibition of Human CYP17 and CYP19 In Vitro

compd	% inhibition[a] CYP17[b]	CYP19[c]	compd	% inhibition[a] CYP17[b]	CYP19[c]
16	<5	39	**23**	26	73
17	25	60	**24**	<5	<5
18	10	45	**25**	21	6
19	<5	92[d]	**26**	5	19
21	28	6	**28**	7	<5
22	51	49	**29**	8	17

[a] Mean value of three experiments, standard deviation usually less than 10%. [b] *E. coli* expressing human CYP17; substrate progesterone, 25 μM; inhibitor concentration, 2.0 μM; ketoconazole, IC_{50} = 2.78 μM. [c] Human placental CYP19; substrate androstenedione, 500 nM; inhibitor concentration, 500 nM; fadrozole, IC_{50} = 30 nM. [d] IC_{50} = 38 nM.

compound within this series. The worst selectivity profile is observed in the case of **19**, inhibiting CYP2C9, CYP2C19, and CYP3A4 with pronounced potency.

Discussion and Conclusion

The inhibitor design concept of the present study triggered the synthesis of compounds **11** and **12** as potential new lead structures by extending a previously established naphthalene molecular scaffold via introduction of a phenyl or benzyl residue in the 3-position. Subsequently, docking studies in our CYP11B2 protein model were performed in order to check for spatial consistency with the pharmacophore hypothesis. It was found that while phenyl-substituted **11** did not dock under the given pharmacophore constraint (Fe(heme)−N(ligand) interaction), benzyl-substituted **12** adequately fits into the binding site by exploiting a previously unexplored subpocket. These findings were confirmed by experimental results, showing that 3-phenyl-substituted pyridylnaphthalene **11** exhibits no significant CYP11B2 inhibition in vitro. In accordance with the docking results, benzyl analogue **12** is a moderately potent aldosterone synthase inhibitor (IC_{50} = 154 nM). The selectivity versus CYP11B1, however, is rather poor with an only six-fold increased IC_{50} value compared to CYP11B2. The lead optimization was accomplished by considering the SAR results obtained previously from the structures of the known CYP11B2 inhibitors, which have been used for the generation of the pharmacophore model (e.g., **1**−**10**). Methoxy substitution in compound **6** afforded the most active compound of the flavone series (IC_{50} = 11 nM) and was therefore chosen as a model substituent to figure out the optimal substituent position in the benzyl moiety of **12**. In the case of the pyridylnaphthalenes, methoxy in the 6-position as accomplished in **2** proved to be favorable in terms of both inhibitory potency and selectivity.[14]

Within the present set of compounds, interesting structure−activity and structure−selectivity relationships can be observed, particularly with regard to the benzyl and the naphthalene

Table 4. Inhibition of Selected Hepatic CYP Enzymes In Vitro

	% inhibition[a]											
	CYP1A2[b,c]		CYP2B6[b,d]		CYP2C9[b,e]		CYP2C19[b,f]		CYP2D6[b,g]		CYP3A4[b,h]	
compd	10 μM	1 μM	10 μM	1 μM	10 μM	1 μM	10 μM	1 μM	10 μM	1 μM	10 μM	1 μM
16	77	23	48	<5	92	51	32	<5	6	<5	79	30
17	83	41	69	24	96	78	87	62	62	23	17	9
19	59	13	61	8	98[i]	96[i]	96	74	7	<5	89	60
28	47	22	43	14	74	35	43	<5	51	23	62	23

[a] Mean value of two experiments, standard deviation usually less than 10%. [b] Recombinantly expressed enzymes from baculovirus-infected insect microsomes (Supersomes). [c] Furafylline, IC_{50} = 2.42 μM. [d] Tranylcypromine, IC_{50} = 6.24 μM. [e] Sulfaphenazole, IC_{50} = 318 nM. [f] Tranylcypromine, IC_{50} = 5.95 μM. [g] Quinidine, IC_{50} = 14 nM. [h] Ketoconazole, IC_{50} = 57 nM. [i] IC_{50} = 64 nM.

moieties. The benzylic part of the investigated molecules represents a pivotal region for structural optimization and is to a great extent dependent on the position of substituents in terms of both inhibitory activity and selectivity toward the highly homologous CYP11B1. Placing methoxy in the *ortho*- or *meta*-position of the benzyl residue significantly reduces the inhibitory potency. Most notably, the inhibition decreases to 24% at an inhibitor concentration of 500 nM in the case of *ortho*-methoxy-derivatized compound **14**. Contrariwise, methoxy in *para*-position as accomplished in compound **16** increases the CYP11B2 activity by a factor of 20 compared to the hydrogen analogue **12** and the selectivity toward CYP11B1 clearly improves (selectivity factor = 359). The experimental observations can be explained by the docking results of compounds **16** and **19**, both bearing a *para*-methoxy group (Figure 3). The introduction of this substituent into the benzyl moiety as accomplished in **16** leads to interactions of the compound with the residues of Pro452, Val339, and Thr279, thus stabilizing the complex formed by coordination of the heme iron by the heterocyclic nitrogen considerably (Figure 3a). In compound **19**, a second methoxy group was introduced at the 6-position of the naphthalene scaffold (Figure 3b). This leads to no additional stabilization of the complex but to a slightly increased selectivity toward CYP11B1. The same trend was observed previously for the binding properties of a series of substituted pyridylnaphthalenes.[14,15] The *para*-cyano and *para*-trifluoromethoxy derivatives **17** and **18** are also highly potent CYP11B2 inhibitors and display IC_{50} values of 2.7 and 3.9 nM, respectively, which corroborates the importance of *para*-substitution for activity. Keeping in mind the high homology of the two CYP11B isoforms, the selectivity factors relating to CYP11B1 inhibition of the latter compounds are particularly noteworthy. Compound **17** displays an approximately 700-fold and compound **18** a 900-fold stronger inhibition of CYP11B2 than of CYP11B1. In the naphthalene molecular scaffold, introduction of a methoxy substituent in the 7-position results in a decreased inhibitory potency (**20**, **30**), whereas the same substituent is readily tolerated in 6-position and even slightly increases the CYP11B1 selectivity in most cases. Figure 4 shows the 6-methoxy substituted derivative **19** mapped to the pharmacophore model. It is obvious that this compound nearly perfectly exploits both the well-known (HY0, HY1, HY2a, AA1, AA2a) and the newly identified (HY3, AA3b) interaction areas, which is reflected by the high inhibitory potency of this compound and underlines the predictive power of our pharmacophore hypothesis. The *para*-methoxy group in the benzyl moiety of **19**,which has been found to be responsible for both high inhibitory activity at CYP11B2 and selectivity toward CYP11B1, fits to the acceptor atom feature AA3b. Hence, targeting this interaction area is a promising strategy in the future design of potent and selective aldosterone synthase inhibitors. With respect to the overall selectivity profile, considering the inhibition of several other CYP enzymes, it becomes apparent that 6-methoxylation endows the benzyl-

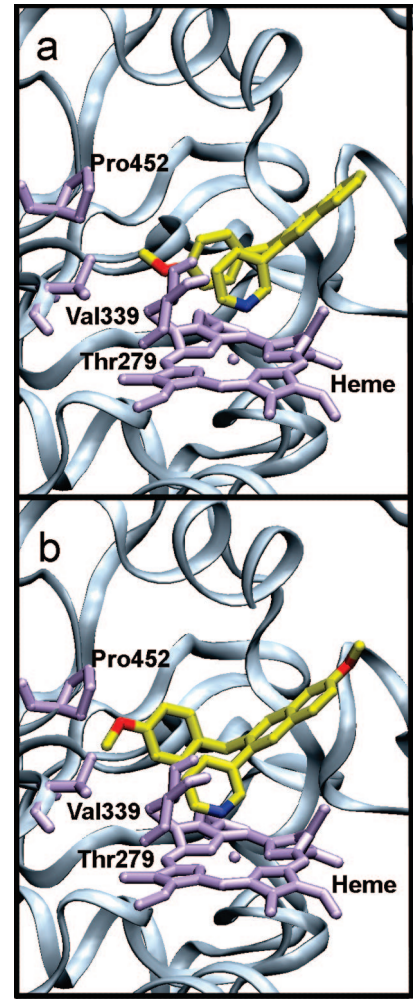

Figure 3. Structure of the CYP11B2 binding pocket with the docked inhibitors **16** (a) and **19** (b). Details of the active site, showing inhibitor, heme cofactor, and the interacting residues of Pro452, Val339, and Thr279.

naphthalenes with an increased inhibitory activity at CYP19 as in the case of compounds **19**, **22**, and **23**, for example, 6-methoxy derivative **19** is a highly potent CYP19 inhibitor displaying an activity similar to that of fadrozole. In addition, the latter compound strongly inhibits several hepatic CYP enzymes (i.e., CYP2C9, CYP2C19, and CYP3A4).

Varying the substitution pattern of the pyridine site induces no distinct changes of the CYP11B2 potency in case of **21** and **22**. Again, 6-methoxylation in compound **22** increases the selectivity versus CYP11B1 compared to **21**. A slightly decreased selectivity toward CYP11B1 can be observed in the case of the isoquinoline derivatives **24** and **25** due to a moderate increase in CYP11B1 potency (IC_{50} < 1000 nM), which corresponds to previously observed results within the pyridyl-

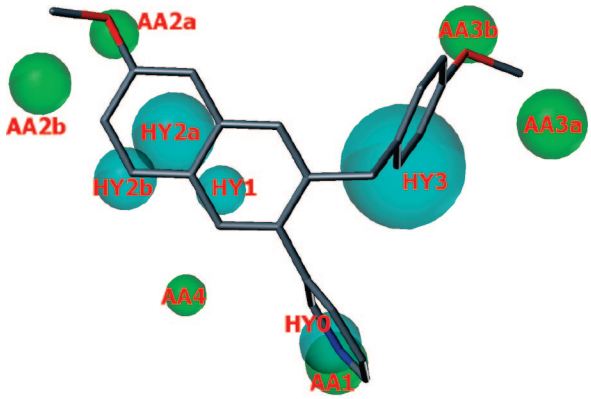

Figure 4. Compound **19** shows an enhanced fit to the pharmacophore hypothesis compared to **1** by additionally exploiting the features HY3 and AA3b. Pharmacophoric features are color-coded: cyan for hydrophobic regions (HY0−HY3) and green for acceptor atom features (AA1−AA4).

naphthalene series.[39] Contrary to the finding that 6-methoxylation effects a slightly improved selectivity (as shown in previous studies[14,15] and observed in case of compounds **13**, **19**, and **22** compared to **12**, **16**, and **21**), the 6-methoxynaphthalene compound **25** is less selective than the hydrogen analogue **24**. Derivatization of the methylene linker in compounds **26**−**35** leads to a decrease in inhibitory potency. The carbonyl analogues **26**, **28**, and **29** are slightly less active than their methylene analogues. On the other hand, CYP11B1 inhibition is reduced to the same degree and the high selectivity is maintained. Again, *para*-trifluoromethoxy has the strongest effect on the inhibitory discrimination between the two CYP11B isoforms and derivative **29** is approximately 400-fold less active at CYP11B1 than at CYP11B2. In the case of the *para*-cyanobenzoyl compound **28**, a decreased inhibition of the sex-hormone producing CYP17, CYP19 as well as the hepatic CYP1A2, CYP2B6, CYP2C9, CYP2C19, and CYP2D6 enzymes is found compared to the benzyl analogue **17**, thus providing an advantageous overall CYP selectivity profile for this compound. Other variations of the methylene moiety as accomplished in the hydroxy- and methoxymethylene derivatives **30**−**35** lead to a pronounced decrease of inhibitory activity compared to the unsubstituted analogues. These compounds display 51−63% inhibition at an inhibitor concentration of 500 nM in case of hydroxy substitution (**30**−**34**) and only 23% in case of methoxy substitution (**35**). Obviously, the decrease in potency with increasing substituent size (hydrogen < carbonyl < hydroxy < methoxy) reflects the increase of steric repulsion between the aryl−aryl spacer and the enzyme parts (i.e., Leu343 and heme cofactor) separating the naphthalene binding site from the subpocket interacting with the benzyl residue.

In summary, it has been shown that our CYP11B2 pharmacophore model has predictive power to identify prospective lead structures. On the basis of the pharmacophore model, a new class of pyridylnaphthalene derivatives with extended carbocyclic skeleton was synthesized. Derivatives with *para*-functionalized benzyl moiety in 3-position of the naphthalene molecular scaffold thoroughly satisfied the spatial constraints imposed by the pharmacophore model and turned out to be highly potent aldosterone synthase inhibitors. The most active compound, *para*-cyanobenzyl derivative **17**, displayed nanomolar potency at the target enzyme (IC_{50} = 2.7 nM). In addition, docking studies using our CYP11B2 protein model proved to be a useful tool to estimate the inhibitory properties of proposed new molecules and to explain structure−activity relationships. The binding behavior of compounds **11** and **12** was adequately predicted by the docking results. Furthermore, it was shown that the high inhibitory potency of the *para*-substituted derivative **16** is due to stabilizing interactions with the residues of Pro452, Val339, and Thr279. The selectivity toward CYP11B1 (up to a factor of 900), which is especially remarkable with respect to the high homology of the two CYP11B isoforms, was found to be a consequence of *para*-substitution and hence of exploiting the AA3b pharmacophoric feature as well. Currently, further studies are underway to evaluate selected compounds for their in vivo properties.

Experimental Section

Chemical and Analytical Methods. Melting points were measured on a Mettler FP1 melting point apparatus and are uncorrected. ^{1}H NMR and ^{13}C spectra were recorded on a Bruker DRX-500 instrument. Chemical shifts are given in parts per million (ppm), and tetramethylsilane (TMS) was used as internal standard for spectra obtained in DMSO-d_6 and $CDCl_3$. All coupling constants (J) are given in Hertz. Mass spectra (LC/MS) were measured on a TSQ Quantum (Thermo Electron Corporation) instrument with a RP18 100-3 column (Macherey Nagel) and with water/acetonitrile mixtures as eluents. Elemental analyses were carried out at the Department of Chemistry, University of Saarbrücken. Reagents were used as obtained from commercial suppliers without further purification. Solvents were distilled before use. Dry solvents were obtained by distillation from appropriate drying reagents and stored over molecular sieves. Flash chromatography was performed on silica gel 40 (35/40−63/70 μM) with petroleum ether/ethyl acetate mixtures as eluents, and the reaction progress was determined by thin-layer chromatography analyses on Alugram SIL G/UV254 (Macherey Nagel). Visualization was accomplished with UV light and $KMnO_4$ solution. All microwave irradiation experiments were carried out in a CEM-Discover monomode microwave apparatus.

The following compounds were prepared according to previously described procedures: 3-(3-methoxynaphthalen-2-yl)pyridine (**11c**),[14] (3-methoxynaphtalene-2-yl)boronic acid (**11d**),[22] methyl 3-methoxynaphthalene-2-carboxylate (**12g**),[26] methyl 3-hydroxynaphthalene-2-carboxylate (**12h**),[25] (3-hydroxynaphthalen-2-yl)(4-methoxyphenyl)-methanone (**26b**),[32] (3-methoxynaphthalen-2-yl)(4-methoxyphenyl)-methanone (**26c**),[32] *N*,4-dimethoxy-*N*-methylbenzamide (**26d**),[32] 4-[(3-hydroxynaphthalen-2-yl)carbonyl]benzonitrile (**28b**),[32] 4-[(3-mehoxynaphthalen-2-yl)carbonyl]benzonitrile (**28c**),[32] 4-cyano-*N*-methoxy-*N*-methylbenzamide (**28d**).[32]

Synthesis of the Target Compounds. Procedure A.[24] Boronic acid (0.75 mmol, 1 equiv), aryl bromide or -triflate (0.9−1.3 equiv), and tetrakis(triphenylphosphane)palladium(0) (43 mg, 37.5 μmol, 5 mol %) were suspended in 1.5 mL of DMF in a 10 mL septum-capped tube containing a stirring magnet. To this was added a solution of $NaHCO_3$ (189 mg, 2.25 mmol, 3 equiv) in 1.5 mL of water, and the vial was sealed with an Teflon cap. The mixture was irradiated with microwaves for 15 min at a temperature of 150 °C with an initial irradiation power of 100 W. After the reaction, the vial was cooled to 40 °C, the crude mixture was partitioned between ethyl acetate and water, and the aqueous layer was extracted three times with ethyl acetate. The combined organic layers were dried over $MgSO_4$, and the solvents were removed in vacuo. The coupling products were obtained after flash chromatography on silica gel (petroleum ether/ethyl acetate mixtures) and/or crystallization. If an oil was obtained, it was dissolved in diethyl ether/methanol and tranferred into the hydrochloride salt by 1N HCl solution in isopropanol/diethyl ether, followed by filtration and optional crystallization from acetone. Analytical data refer to the free base unless otherwise noted.

Procedure B. Boronic acid (1 equivalent), aryl bromide or -triflate (1.3−1.5 equiv), and tetrakis(triphenylphosphane)palladium(0) (5 mol %) were suspended in toluene/ethanol 4/1 to give a 0.07−0.1 M solution of boronic acid under an atosphere of nitrogen. To this was added a 1N aqueous solution of Na_2CO_3 (6

equivalents). The mixture was then refluxed for 12−18 h, cooled to room temperature, diluted with water, and extracted several times with ethyl acetate. The combined extracts were dried over $MgSO_4$, concentrated, and purified by flash chromatography on silica gel (petroleum ether/ethyl acetate mixtures) and/or crystallization. If an oil was obtained, it was dissolved in diethyl ether/methanol and transferred into the hydrochloride salt by 1N HCl solution in isopropanol/diethyl ether, followed by filtration and optional crystallization from acetone. Analytical data refer to the free base unless otherwise noted.

Procedure C.[33,34] To a 0.6 M solution of NaI (6 equiv) in acetonitrile was added chlorotrimethylsilane (6 equiv) at room temperature, and the mixture was stirred for 30 min before cooling to 0 °C with an ice−water bath. Then, a 1 M solution of the phenylnaphthylalcohol (1 equiv) in acetonitrile was added dropwise. After complete addition, the mixture was heated at 55 °C for 3 h. After recooling to room temperature, the reaction was quenched by addition of saturated aqueous $NaHCO_3$ solution. The layers were separated, and the aqueous layer extracted twice with ethyl acetate The combined organic layers were washed with a solution of $Na_2S_2O_3$, water, and brine. The extracts were dried over $MgSO_4$, concentrated, and purified by flash chromatography on silica gel (petroleum ether/ethyl acetate mixtures). If an oil was obtained, it was dissolved in diethyl ether/methanol and tranferred into the hydrochloride salt by 1N HCl solution in isopropanol/diethyl ether, followed by filtration and optional crystallization from acetone. Analytical data refer to the free base unless otherwise noted.

Procedure D. To a 0.05 M solution of benzoylnaphthalene in dry methanol was added sodium borohydride (2 equiv) at such a rate as to maintain the internal reaction temperature below 5 °C. The reaction mixture was stirred for 1 h, diluted with diehtylether, and treated with saturated aqueous $NaHCO_3$ solution. The mixture was then extracted three times with ethyl acetate, washed twice with saturated aqueous $NaHCO_3$ solution and once with brine, and dried over $MgSO_4$. The filtrate was concentrated in vacuo, and the residue was flash chromatographed on silica gel (petroleum ether/ethyl acetate mixtures) to afford the corresponding alcohols.

3-(3-Phenylnaphthalen-2-yl)pyridine (11). The compound was obtained according to procedure A from **11a** (657 mg, 1.86 mmol) and phenylboronic acid (854 mg, 4.00 mmol) after flash chromatography on silica gel (petroleum ether/ethyl acetate, 7/3, $R_f = 0.22$) as a colorless oil (195 mg, 0.69 mmol, 37%). Precipitation of the hydrochloride salt afforded a highly hygroscopic solid, mp (HCl salt) 106−109 °C. MS *m/z* 282.70 (MH^+). Anal. ($C_{21}H_{15}N \cdot HCl \cdot 1.5H_2O$) C, H, N.

3-(3-Benzylnaphthalen-2-yl)pyridine (12). The compound was obtained according to procedure A from **12a** (433 mg, 1.18 mmol) and 3-pyridineboronic acid (105 mg, 0.85 mmol) after flash chromatography on silica gel (petroleum ether/ethyl acetate, 4/1, $R_f = 0.19$) as a colorless oil (186 mg, 0.63 mmol, 74%), mp (HCl salt) 197−198 °C. MS *m/z* 296.14 (MH^+). Anal. ($C_{22}H_{17}N \cdot HCl \cdot 0.6H_2O$) C, H, N.

3-(3-Benzyl-6-methoxynaphthalen-2-yl)pyridine (13). The compound was obtained according to procedure A from **13a** (462 mg, 1.17 mmol) and 3-pyridineboronic acid (100 mg, 0.81 mmol) after flash chromatography on silica gel (petroleum ether/ethyl acetate, 4/1, $R_f = 0.18$) as a colorless oil (196 mg, 0.60 mmol, 74%), mp (HCl salt) 170−172 °C. MS *m/z* 326.09 (MH^+). Anal. ($C_{23}H_{19}NO \cdot HCl \cdot 0.6H_2O$) C, H, N.

3-[3-(2-Methoxybenzyl)naphthalen-2-yl]pyridine (14). The compound was obtained according to procedure A from **14a** (462 mg, 1.17 mmol) and 3-pyridineboronic acid (100 mg, 0.81 mmol) after flash chromatography on silica gel (petroleum ether/ethyl acetate, 7/3, $R_f = 0.26$) as colorless oil (161 mg, 0.50 mmol, 61%), mp (HCl salt) 214−216 °C. MS *m/z* 326.02 (MH^+). Anal. ($C_{23}H_{19}NO \cdot HCl \cdot 0.6H_2O$) C, H, N.

3-[3-(3-Methoxybenzyl)naphthalen-2-yl]pyridine (15). The compound was obtained according to procedure A from **15a** (433 mg, 1.09 mmol) and 3-pyridineboronic acid (92 mg, 0.75 mmol) after flash chromatography on silica gel (petroleum ether/ethyl acetate, 4/1, $R_f = 0.13$) as a colorless oil (162 mg, 0.50 mmol, 66%), mp (HCl salt) 161−162 °C. MS *m/z* 326.02 (MH^+). Anal. ($C_{23}H_{19}NO \cdot HCl \cdot 0.6H_2O$) C, H, N.

3-[3-(4-Methoxybenzyl)naphthalen-2-yl]pyridine (16). The compound was obtained according to procedure A from **16a** (476 mg, 1.20 mmol) and 3-pyridineboronic acid (92 mg, 0.75 mmol) after flash chromatography on silica gel (petroleum ether/ethyl acetate, 4/1, $R_f = 0.14$) as a colorless oil (199 mg, 0.56 mmol, 75%), mp (HCl salt) 180−182 °C. ^{1}H NMR (500 MHz, $CDCl_3$): $\delta = 3.75$ (s, 3H), 4.00 (s, 2H), 6.72 (d, $^3J = 8.8$ Hz, 2H), 6.82 (d, $^3J = 8.8$ Hz, 2H), 7.26 (ddd, $^3J = 7.9$ Hz, $^3J = 4.7$ Hz, $^5J = 0.9$ Hz, 1H), 7.45−7.52 (m, 3H), 7.68 (s, 1H), 7.70 (s, 1H), 7.79−7.83 (m, 2H), 8.55 (dd, $^4J = 2.2$ Hz, $^5J = 0.9$ Hz, 1H), 8.59 (dd, $^3J = 4.7$ Hz, $^4J = 1.9$ Hz, 1H). ^{13}C NMR (125 MHz, $CDCl_3$): $\delta = 39.0$, 55.2, 113.7, 122.7, 126.0, 126.4, 127.3, 127.6, 128.9, 129.4, 129.7, 132.0, 132.4, 133.1, 136.6, 137.06, 137.13, 148.2, 149.9, 157.9. MS *m/z* 326.16 (MH^+). Anal. ($C_{23}H_{19}NO \cdot HCl \cdot 0.6H_2O$) C, H, N.

4-(3-Pyridin-3-yl-naphthalen-2-ylmethyl)benzonitrile (17). The compound was obtained according to procedure C from **33** (841 mg, 2.50 mmol), sodium iodide (2.25 g, 15.0 mmol), and chlorotrimethylsilane (1.63 g, 15.0 mmol) after flash chromatography on silica gel (petroleum ether/ethyl acetate, 7/3, $R_f = 0.15$) as a colorless oil (486 mg, 1.52 mmol, 61%), mp (HCl salt) 130−131 °C. MS *m/z* 321.33 (MH^+). Anal. ($C_{23}H_{16}N_2 \cdot HCl \cdot 0.8H_2O$) C, H, N.

3-[3-(4-Trifluoromethoxybenzyl)naphthalen-2-yl]pyridine (18). The compound was obtained according to procedure C from **34** (395 mg, 1.00 mmol), sodium iodide (899 mg, 6.0 mmol), and chlorotrimethylsilane (652 mg, 6.0 mmol) after flash chromatography on silica gel (petroleum ether/ethyl acetate, 4/1, $R_f = 0.28$) as a colorless oil (292 mg, 0.77 mmol, 77%). Precipitation of the hydrochloride salt afforded a highly hygroscopic solid, mp (HCl salt) 139−142 °C. MS *m/z* 379.90 (MH^+). Anal. ($C_{24}H_{17}F_3NO \cdot HCl \cdot 0.2H_2O$) C, H, N.

3-[6-Methoxy-3-(4-methoxybenzyl)naphthalen-2-yl]pyridine (19). The compound was obtained according to procedure A from **19a** (512 mg, 1.20 mmol) and 3-pyridineboronic acid (113 mg, 0.92 mmol) after flash chromatography on silica gel (petroleum ether/ethyl acetate, 7/3, $R_f = 0.18$) as a colorless oil (189 mg, 0.55 mmol, 60%), mp (HCl salt) 114−115 °C. ^{1}H NMR (500 MHz, $CDCl_3$): $\delta = 3.75$ (s, 3H), 3.91 (s, 3H), 3.98 (s, 2H), 6.73 (d, $^3J = 8.5$ Hz, 2H), 6.84 (d, $^3J = 8.5$ Hz, 2H), 7.09 (d, $^4J = 2.5$ Hz, 1H), 7.13 (dd, $^3J = 9.0$ Hz, $^4J = 2.5$ Hz, 1H), 7.25 (dd, $^3J = 8.0$ Hz, $^3J = 4.8$ Hz, 1H), 7.51 (m, 1H), 7.57 (s, 1H), 7.60 (s, 1H), 7.71 (d, $^3J = 8.9$ Hz, 1H), 8.54 (d, $^4J = 1.9$ Hz, 1H), 8.56 (dd, $^3J = 4.8$ Hz, $^4J = 1.5$ Hz, 1H). ^{13}C NMR (125 MHz, $CDCl_3$): $\delta = 38.9$, 55.2, 55.3, 105.2, 113.7, 119.0, 122.8, 127.5, 127.8, 129.1, 129.2, 129.8, 132.6, 134.4, 134.8, 136.8, 137.3, 137.6, 148.1, 150.1, 157.9, 158.1. MS *m/z* 356.25 (MH^+). Anal. ($C_{24}H_{21}NO_2 \cdot HCl \cdot 0.8H_2O$) C, H, N.

3-[7-Methoxy-3-(4-methoxybenzyl)naphthalen-2-yl]pyridine (20). The compound was obtained according to procedure C from **20a** (400 mg, 1.08 mmol), sodium iodide (1.65 g, 11.0 mmol), and chlorotrimethylsilane (1.20 g, 11.0 mmol) after flash chromatography on silica gel (petroleum ether/ethyl acetate, 7/3, $R_f = 0.11$) as a colorless oil (148 mg, 0.42 mmol, 39%), mp (HCl salt) 101−103 °C. MS *m/z* 356.04 (MH^+). Anal. ($C_{24}H_{21}NO_2 \cdot HCl \cdot 0.1H_2O$) C, H, N.

3-Methoxy-5-[3-(4-methoxybenzyl)naphthalen-2-yl]pyridine (21). The compound was obtained according to procedure A from **16a** (396 mg, 1.00 mmol) and 5-methoxy-3-pyridineboronic acid (130 mg, 0.85 mmol) after flash chromatography on silica gel (petroleum ether/ethyl acetate, 7/3, $R_f = 0.21$) as a colorless oil (149 mg, 0.42 mmol, 49%), mp (HCl salt) 106−108 °C. MS *m/z* 356.09 (MH^+). Anal. ($C_{24}H_{21}NO_2 \cdot HCl \cdot 0.5H_2O$) C, H, N.

3-Methoxy-5-[6-methoxy-3-(4-methoxybenzyl)naphthalen-2-yl]pyridine (22). The compound was obtained according to procedure A from **19a** (426 mg, 1.00 mmol) and 5-methoxy-3-pyridineboronic acid (130 mg, 0.85 mmol) after flash chromatography on silica gel (petroleum ether/ethyl acetate, 7/3, $R_f = 0.18$) as colorless plates (244 mg, 0.63 mmol, 75%), mp 129−130 °C. MS *m/z* 385.91 (MH^+). Anal. ($C_{25}H_{23}NO_3$) C, H, N.

3-(3-Benzyl-6-methoxynaphthalen-2-yl)5-methoxypyridine (23). The compound was obtained according to procedure A from **13a** (396 mg, 1.00 mmol) and 5-methoxy-3-pyridineboronic acid acid (130 mg, 0.85 mmol) after flash chromatography on silica gel (petroleum ether/ethyl acetate, 7/3, $R_f = 0.21$) as a colorless oil (221 mg, 0.62 mmol, 73%), mp (HCl salt) 119−121 °C. MS *m/z* 356.09 (MH^+). Anal. ($C_{24}H_{21}NO_2 \cdot HCl \cdot 0.2H_2O$) C, H, N.

4-[3-(4-Methoxybenzyl)naphthalen-2-yl]isoquinoline (24). The compound was obtained according to procedure A from **16a** (396 mg, 1.00 mmol) and 4-isoquinolineboronic acid (130 mg, 0.75 mmol) after flash chromatography on silica gel (petroleum ether/ethyl acetate, 7/3, $R_f = 0.20$) as a colorless oil (178 mg, 0.47 mmol, 63%), mp (HCl salt) 202−203 °C. MS *m/z* 376.12 (MH^+). Anal. ($C_{27}H_{21}NO \cdot HCl \cdot 0.5H_2O$) C, H, N.

4-[6-Methoxy-3-(4-methoxybenzyl)naphthalen-2-yl]isoquinoline (25). The compound was obtained according to procedure A from **19a** (456 mg, 1.07 mmol) and 4-isoquinolineboronic acid (130 mg, 0.75 mmol) after flash chromatography on silica gel (petroleum ether/ethyl acetate, 7/3, $R_f = 0.18$) and crystallization from acetone/diethyl ether as colorless plates (178 mg, 0.44 mmol, 59%), mp 158−159 °C. MS *m/z* 406.00 (MH^+). Anal. ($C_{28}H_{23}NO_2$) C, H, N.

(4-Methoxyphenyl)(3-pyridin-3-yl-naphthalen-2-yl)methanone (26). The compound was obtained according to procedure B from **26a** (4.02 g, 9.80 mmol) and 3-pyridineboronic acid (1.02 g, 8.33 mmol) after flash chromatography on silica gel (petroleum ether/ethyl acetate, 1/1, $R_f = 0.22$) as an off-white solid (2.66 g, 7.84 mmol, 94%), mp 69−72 °C. MS *m/z* 340.07 (MH^+). Anal. ($C_{23}H_{17}NO_2 \cdot 0.2H_2O$) C, H, N.

(3-Fluoro-4-methoxyphenyl)(3-pyridin-3-yl-naphthalen-2-yl)-methanone (27). The compound was obtained according to procedure B from **27a** (4.19 g, 9.78 mmol) and 3-pyridineboronic acid (1.02 g, 8.33 mmol) after flash chromatography on silica gel (petroleum ether/ethyl acetate, 1/1, $R_f = 0.16$) as an off-white solid (2.52 g, 7.05 mmol, 85%), mp 96−97 °C. MS *m/z* 358.00 (MH^+). Anal. ($C_{23}H_{16}FNO_2 \cdot 0.1H_2O$) C, H, N.

4-(3-Pyridin-3-yl-naphthalene-2-carbonyl)benzonitrile (28). The compound was obtained according to procedure B from **28a** (3.0 g, 7.40 mmol) and 3-pyridineboronic acid (1.0 g, 8.20 mmol) after flash chromatography on silica gel (petroleum ether/ethyl acetate, 7/3, $R_f = 0.15$) as yellowish needles (1.67 g, 5.0 mmol, 68%), mp 135−136 °C. MS *m/z* 335.05 (MH^+). Anal. ($C_{23}H_{14}N_2O \cdot 0.1H_2O$) C, H, N.

(3-Pyridin-3-yl-naphthalen-2-yl)(4-trifluoromethoxyphenyl)-methanone (29). The compound was obtained according to procedure B from **29a** (4.57 g, 9.84 mmol) and 3-pyridineboronic acid (1.02 g, 8.33 mmol) after flash chromatography on silica gel (petroleum ether/ethyl acetate, 7/3, $R_f = 0.20$) as a colorless oil (3.20 g, 8.14 mmol, 98%). Precipitation of the hydrochloride salt afforded a highly hygroscopic solid, mp (HCl salt) 116−118 °C. MS *m/z* 393.89 (MH^+). Anal. ($C_{23}H_{14}F_3NO_2 \cdot HCl$) C, H, N.

(4-Methoxyphenyl)(6-methoxy-3-pyridin-3-yl-naphthalen-2-yl)methanone (30). The compound was obtained according to procedure B from **30a** (1.54 g, 3.50 mmol) and 3-pyridineboronic acid (374 mg, 3.0 mmol) after flash chromatography on silica gel (petroleum ether/ethyl acetate, 1/1, $R_f = 0.08$) and crystallization from methanol as a white solid (723 mg, 1.96 mmol, 65%), mp 140−141 °C. MS *m/z* 370.10 (MH^+). Anal. ($C_{24}H_{19}NO_3 \cdot 0.2H_2O$) C, H, N.

(4-Methoxyphenyl)(3-pyridin-3-yl-naphthalen-2-yl)methanol (31). The compound was obtained according to pocedure D from **26** (1.02 g, 3.0 mmol) and sodium borohydride (226 mg, 6.0 mmol) after flash chromatography on silica gel (petroleum ether/ethyl acetate, 1/1, $R_f = 0.18$) as a colorless solid (597 mg, 1.75 mmol, 58%), mp 77−78 °C. MS *m/z* 342.10 (MH^+). Anal. ($C_{23}H_{19}NO_2 \cdot 0.3H_2O$) C, H, N.

(3-Fluoro-4-methoxyphenyl)(3-pyridin-3-yl-naphthalen-2-yl)-methanol (32). The compound was obtained according to procedure D from **27** (2.11 g, 5.91 mmol) and sodium borohydride (246 mg, 6.50 mmol) after flash chromatography on silica gel (petroleum ether/ethyl acetate, 1/1, $R_f = 0.19$) as a yellowish solid (543 mg, 1.51 mmol, 26%), mp 75−76 °C. MS *m/z* 359.96 (MH^+). Anal. ($C_{23}H_{18}FNO_2 \cdot 0.5H_2O$) C, H, N.

4-[Hydroxy-(3-pyridin-3-yl-naphthalen-2-yl)methyl]benzonitrile (33). The compound was obtained according to procedure D from **28** (1.46 g, 4.37 mmol) and sodium borohydride (182 mg, 4.80 mmol) after flash chromatography on silica gel (petroleum ether/ethyl acetate, 1/1, $R_f = 0.16$) as a colorless solid (1.22 g, 3.63 mmol, 83%), mp 101−103 °C. MS *m/z* 336.93 (MH^+). Anal. ($C_{23}H_{16}N_2O \cdot 0.5H_2O$) C, H, N.

(3-Pyridin-3-yl-naphthalen-2-yl)(4-trifluoromethoxyphenyl)-methanol (34). The compound was obtained according to procedure D from **29** (2.80 g, 7.12 mmol) and sodium borohydride (295 mg, 7.80 mmol) after flash chromatography on silica gel (petroleum ether/ethyl acetate, 1/1, $R_f = 0.32$) as a colorless solid (1.86 g, 4.70 mmol, 66%), mp 65−66 °C. MS *m/z* 396.20 (MH^+). Anal. ($C_{23}H_{16}F_3NO_2 \cdot 0.2H_2O$) C, H, N.

3-{3-[Methoxy-(4-methoxyphenyl)methyl]naphthalen-2-yl}pyridine (35). To a suspension of NaH (40 mg, 1.0 mmol, 60% dispersion in oil) in 5 mL dry THF at was added dropwise a solution of **31** (300 mg, 0.88 mmol) in 5 mL of THF at room temperature under an atmosphere of nitrogen. After hydrogen evolution ceased, a solution of methyliodide (59 μL, 0.95 mmol) in 5 mL of THF was added dropwise, and the resulting mixture was stirred for 5 h at room temperature. After 2 h, an additional 59 μL of methyliodide was added. The mixture was then treated with saturated aqueous NH_4Cl solution and extracted three times with ethyl acetate. The combined organic layers were washed with water and brine, dried over $MgSO_4$, and the solvent was evaporated in vacuo. **35** was obtained after flash chromatography on silica gel (petroleum ether/ethyl acetate, 1/1, $R_f = 0.39$) as colorless oil (226 mg, 0.64 mmol, 72%), mp (HCl salt) 113−114 °C. MS *m/z* 356.11 (MH^+). Anal. ($C_{24}H_{21}NO_2 \cdot HCl \cdot 0.7H_2O$) C, H, N.

Biological Methods. 1. Enzyme preparations. CYP17 and CYP19 preparations were obtained by described methods: the 50000*g* sediment of *E. coli* expressing human CYP17[40] and microsomes from human placenta for CYP19.[42] 2. Enzyme assays. The following enzyme assays were performed as previously described: CY17[40] and CYP19.[42] 3. Activity and selectivity assay using V79 cells. V79 MZh 11B1 and V79 MZh 11B2 cells[36] were incubated with [4-^{14}C]-11-deoxycorticosterone as substrate and inhibitor in at least three different concentrations. The enzyme reactions were stopped by addition of ethyl acetate. After vigorous shaking and a centrifugation step (10000*g*, 2 min), the steroids were extracted into the organic phase, which was then separated. The conversion of the substrate was analyzed by HPTLC and a phosphoimaging system as described.[10,36] 4. Inhibition of human hepatic CYP enzymes. The recombinantly expressed enzymes from baculovirus-infected insect microsomes (Supersomes) were used and the manufacturer's instructions (www.gentest.com) were followed.

Computational Methods. 1. Pharmacophore modeling. The most potent compounds of the heteroaryl substituted methyleneindane and naphthalene derivatives and the most potent flavones were selected as training set (see Supporting Information for composition of the training set) for the generation of an extended pharmacophore model. GALAHAD,[19] the pharmacophore generation module of SYBYL 7.3.2 (Sybyl, Tripos Inc., St. Louis, MO), was used to generate pharmacophore hypotheses of the series of inhibitors form hypermolecules incorporating the structural information of the data set and alignments from sets of ligand molecules. In the genetic algorithm, default values were used. In the present case, 100 models were generated and the best 20 pharmacophore hypotheses were saved. GALAHAD takes into account energetics, steric similarity, and pharmacophoric overlap while accommodating conformational flexibility, ambiguous stereochemistry, alternative ring configurations, multiple partial match constraints, and alternative feature mappings among molecules. All the other molecules of the library were then aligned using each of the 20 pharmacophores as a template, and the best pharmacophore was selected. The top ranked model was the best in three of the most indicative ranking criteria of the used software (Pareto ranking,[20] Specificity, and Mol-query).

An additional donor site feature (not shown in the figures) was manually added to simulate the complexation of the heme iron by the sp^2-hybridized nitrogen (AA1) in order to fix the orientation of the lone pair of the sp^2-hybridized nitrogen. This refined pharmacophore model was selected as molecular query for the alignment of our database library. The core of the pharmacophoric scheme is formed by five hydrophobic features (HY0, HY1, HY2a, HY2b) and the acceptor atom (AA) spheres represent the H-bond acceptors. In some cases, the acceptor feature AA2a overlapped a donor feature (data not shown), indicating the presence of an OH function. The final pharmacophore model consists of 12 pharmacophoric features: four essential ones (HY0, AA1, HY1), necessary for basal inhibitory potency, and eight partial matches (HY2, HY2b, AA2a, AA2b, HY3, AA3a, AA3b, and AA4). 2. Protein modeling and docking. Using the resolved human cytochrome CYP2C9 structure (PDB code: 1OG5)[43] as template, a homology model was build and refined for CYP11B2. This work has been described in more detail by our group in four recent papers.[12−15] In this study, selected compounds were docked into the refined homology model using FlexX-Pharm.[44] A pharmacophore constraint was applied to ensure the right binding mode of the inhibitors with the heme cofactor. For this purpose, the standard Fe−N interaction parameters of FlexX[45,46] were modified and a directed heme-Fe−N interaction was defined perpendicular to the heme plane. The constraint requires the existence of an inhibitor nitrogen atom on the surface of an interaction cone with a 20° radius, which has its origin at the Fe atom and points perpendicular to the heme plane (with a length of 2.2 Å). Only docking solutions were accepted, which fulfill this constraint. For all other ligand−protein interactions, the standard FlexX interaction parameters and geometries were used. The protein−ligand interactions were analyzed using the FlexX software.

Acknowledgment. We thank Gertrud Schmitt and Jeannine Jung for their help in performing the in vitro tests. The investigation of the hepatic CYP profile by Dr. Ursula Müller-Viera, Pharmacelsus CRO, Saarbrücken, is highly appreciated. S.L. is grateful to Saarland University for a scholarship (Landesgraduierten-Förderung). Thanks are due to Prof. J. J. Rob Hermans, University of Maastricht, The Netherlands, for supplying the V79 CYP11B1 cells, and Prof. Rita Bernhardt, Saarland University, for supplying the V79 CYP11B2 cells.

Supporting Information Available: Additional inhibitory data of compounds **1**−**10** (CYP11B1 inhibition and selectivity factors), NMR spectroscopic data of the target compounds **11**−**15**, **17**, **18**, **20**−**35**, full experimental details and spectroscopic characterization of the reaction intermediates **11a**−**16a**, **19a**, **20a**, **26a**−**30a**, **11b**−**16b**, **19b**, **26b**−**30b**, **11c**−**16c**, **19c**, **11d**−**16d**, **19d**, **26d**−**30d**, **12e**−**14e**, **12f**−**14f**, **12g**−**14g**, **12h**, **13h**, elemental analysis results and purity data (LC/MS) of compounds **11**−**35**, pharmacophore modeling training set and pharmacophore geometric properties. This material is available free of charge via the Internet at http://pubs.acs.org.

References

(1) Kawamoto, T.; Mitsuuchi, Y.; Toda, K.; Yokoyama, Y.; Miyahara, K.; Miura, S.; Ohnishi, T.; Ichikawa, Y.; Nakao, K.; Imura, H.; Ulick, S.; Shizuta, Y. Role of steroid 11β-hydroxylase and steroid 18-hydroxylase in the biosynthesis of glucocorticoids and mineralocorticoids in humans. *Proc. Natl. Acad. Sci. U.S.A.* **1992**, *89*, 1458–1462.

(2) (a) Brilla, C. G. Renin−angiotensin−aldosterone system and myocardial fibrosis. *Cardiovasc. Res.* **2000**, *47*, 1–3. (b) Lijnen, P.; Petrov, V. Induction of cardiac fibrosis by aldosterone. *J. Mol. Cell. Cardiol.* **2000**, *32*, 865–879.

(3) (a) Struthers, A. D. Aldosterone escape during angiotensin-converting enzyme inhibitor therapy in chronic heart failure. *J. Card. Fail.* **1996**, *2*, 47–54. (b) Sato, A.; Saruta, T. Aldosterone escape during angiotensin-converting enzyme inhibitor therapy in essential hypertensive patients with left ventricular hypertrophy. *J. Int. Med. Res.* **2001**, *29*, 13–21.

(4) Pitt, B.; Zannad, F.; Remme, W. J.; Cody, R.; Castaigne, A.; Perez, A.; Palensky, J.; Wittes, J. The effect of spironolactone on morbidity and mortality in patients with severe heart failure. *N. Engl. J. Med.* **1999**, *341*, 709–717.

(5) Pitt, B.; Remme, W.; Zannad, F.; Neaton, J.; Martinez, F.; Roniker, B.; Bittman, R.; Hurley, S.; Kleiman, J.; Gatlin, M. Eplerenone, a selective aldosterone blocker, in patients with left ventricular dysfunction after myocardial infarction. *N. Eng. J. Med.* **2003**, *348*, 1309–1321.

(6) Delcayre, C.; Swynghedauw, B. Molecular mechanisms of myocardial remodeling. The role of aldosterone. *J. Mol. Cell. Cardiol.* **2002**, *34*, 1577–1584.

(7) (a) Wehling, M. Specific, nongenomic actions of steroid hormones. *Annu. Rev. Physiol.* **1997**, *59*, 365–393. (b) Lösel, R.; Wehling, M. Nongenomic actions of steroid hormones. *Nat. Rev. Mol. Cell. Biol.* **2003**, *4*, 46–55.

(8) Chai, W.; Garrelds, I. M.; de Vries, R.; Batenburg, W. W.; van Kats, J. P.; Danser, A. H. J. Nongenomic effects of aldosterone in the human heart: interaction with angiotensin II. *Hypertension* **2005**, *46*, 701–706.

(9) Hartmann, R. W. Selective inhibition of steroidogenic P450 enzymes: Current status and future perspectives. *Eur. J. Pharm. Sci.* **1994**, *2*, 15–16.

(10) Ehmer, P. B.; Bureik, M.; Bernhardt, R.; Müller, U.; Hartmann, R. W. Development of a test system for inhibitors of human aldosterone synthase (CYP11B2): screening in fission yeast and evaluation of selectivity in V79 cells. *J. Steroid Biochem. Mol. Biol.* **2002**, *81*, 173–179.

(11) Hartmann, R. W.; Müller, U.; Ehmer, P. B. Discovery of selective CYP11B2 (aldosterone synthase) inhibitors for the therapy of congestive heart failure and myocardial fibrosis. *Eur. J. Med. Chem.* **2003**, *38*, 363–366.

(12) Ulmschneider, S.; Müller-Vieira, U.; Mitrenga, M.; Hartmann, R. W.; Oberwinkler-Marchais, S.; Klein, C. D.; Bureik, M.; Bernhardt, R.; Antes, I.; Lengauer, T. Synthesis and evaluation of imidazolylmethylenetetrahydronaphthalenes and imidazolylmethyleneindanes: potent inhibitors of aldosterone synthase. *J. Med. Chem.* **2005**, *48*, 1796–1805.

(13) Ulmschneider, S.; Müller-Vieira, U.; Klein, C. D.; Antes, I.; Lengauer, T.; Hartmann, R. W. Synthesis and evaluation of (pyridylmethylene) tetrahydronaphthalenes/-indanes and structurally modified derivatives: potent and selective inhibitors of aldosterone synthase. *J. Med. Chem.* **2005**, *48*, 1563–1575.

(14) Voets, M.; Antes, I.; Scherer, C.; Müller-Vieira, U.; Biemel, K.; Barassin, C.; Oberwinkler-Marchais, S.; Hartmann, R. W. Heteroaryl substituted naphthalenes and structurally modified derivatives: selective inhibitors of CYP11B2 for the treatment of congestive heart failure and myocardial fibrosis. *J. Med. Chem.* **2005**, *48*, 6632–6642.

(15) Voets, M.; Antes, I.; Scherer, C.; Müller-Vieira, U.; Biemel, K.; Oberwinkler-Marchais, S.; Hartmann, R. W. Synthesis and evaluation of heteroaryl-substituted dihydronaphthalenes and indenes: potent and selective inhibitors of aldosterone synthase (CYP11B2) for the treatment of congestive heart failure and myocardial fibrosis. *J. Med. Chem.* **2006**, *49*, 2222–2231.

(16) Taymans, S. E.; Pack, S.; Pak, E.; Torpy, D. J.; Zhuang, Z.; Stratakis, C. A. Human CYP11B2 (aldosterone synthase) maps to chromosome 8q24.3. *J. Clin. Endocrinol. Metab.* **1998**, *83*, 1033–1036.

(17) (a) Cavalli, A.; Bisi, A.; Bertucci, C.; Rosini, C.; Paluszcak, A.; Gobbi, S.; Giorgio, E.; Rampa, A.; Belluti, F.; Piazzi, L.; Valenti, P.; Hartmann, R. W.; Recanatini, M. Enantioselective nonsteroidal aromatase inhibitors identified through a multidisciplinary medicinal chemistry approach. *J. Med. Chem.* **2005**, *48*, 7282–7289. (b) Gobbi, S.; Cavalli, A.; Rampa, A.; Belluti, F.; Piazzi, L.; Paluszcak, A.; Hartmann, R. W.; Recanatini, M.; Bisi, A. Lead optimization providing a series of flavone derivatives as potent nonsteroidal inhibitors of the cytochrome P450 aromatase enzyme. *J. Med. Chem.* **2006**, *49*, 4777–4780.

(18) Ulmschneider, S.; Negri, M.; Voets, M.; Hartmann, R. W. Development and evaluation of a pharmacophore model for inhibitors of aldosterone synthase (CYP11B2). *Bioorg. Med. Chem. Lett.* **2006**, *16*, 25–30.

(19) (a) Richmond, N. J.; Abrams, C. A.; Wolohan, P. R.; Abrahamian, E.; Willett, P.; Clark, R. D. GALAHAD: 1. Pharmacophore identification by hypermolecular alignment of ligands in 3D. *J. Comput.-Aided Mol. Des.* **2006**, *20*, 567–587. (b) Shepphird, J. K.; Clark, R. D. A marriage made in torsional space: Using GALAHAD models to drive pharmacophore multiplet searches. *J. Comput. Aided Mol. Des.* **2006**, *20*, 763–771.

(20) Gillet, V. J.; Willett, P.; Fleming, P. J.; Green, D. V. S. Designing focused libraries using MoSELECT. *J. Mol. Graph. Model.* **2003**, *20*, 491–498.

(21) Miyaura, N.; Suzuki, A. Palladium-catalyzed cross-coupling reactions of organoboron compounds. *Chem. Rev.* **1995**, *95*, 2457–2483.

(22) Chowdhury, S.; Georghiou, P. E. Synthesis and properties of a new member of the calixnaphthalene family: A C2-symmetrical endo-calix[4]naphthalene. *J. Org. Chem.* **2002**, *67*, 6808–6811.
(23) Bengtson, A.; Hallberg, A.; Larhed, M. Fast synthesis of aryl triflates with controlled microwave heating. *Org. Lett.* **2002**, *4*, 1231–1233.
(24) Appukkuttan, P.; Orts, A. B.; Chandran, R. P.; Goeman, J. L.; van der Eycken, J.; Dehaen, W.; van der Eycken, E. Generation of a small library of highly electron-rich 2-(hetero)aryl-substituted phenethylamines by the Suzuki−Miyaura reaction: A short synthesis of an apogalanthamine analogue. *Eur. J. Org. Chem.* **2004**, 3277–3285.
(25) Miller, L. E.; Hanneman, W. W.; St. John, W. L.; Smeby, R. R. The reactivity of the methyl group in 2-methyl-3-nitronaphthalene. *J. Am. Chem. Soc.* **1954**, *76*, 296–297.
(26) Wu, K.-C.; Lin, Y.-S.; Yeh, Y.-S.; Chen, C.-Y.; Ahmed, M. O.; Chou, P.-T.; Hon, Y.-S. Design and synthesis of intramolecular hydrogen bonding systems. Their application in metal cation sensing based on excited-state proton transfer reaction. *Tetrahedron* **2004**, *60*, 11861–11868.
(27) Brown, H. C.; Narasimhan, S.; Choi, Y. M. Selective reductions. 30. Effect of cation and solvent on the reactivity of saline borohydrides for reduction of carboxylic esters. Improved procedures for the conversion of esters to alcohols by metal borohydrides. *J. Org. Chem.* **1982**, *47*, 4702–4708.
(28) Einhorn, J.; Einhorn, C.; Ratajczak, F.; Pierre, J.-L. Efficient and highly selective oxidation of primary alcohols to aldehydes by *N*-chlorosuccinimide mediated by oxoammonium salts. *J. Org. Chem.* **1996**, *61*, 7452–7454.
(29) Parikh, J. R.; Doering, W. v. E. Sulfur trioxide in the oxidation of alcohols by dimethyl sulfoxide. *J. Am. Chem. Soc.* **1967**, *89*, 5505–5507.
(30) Ono, A.; Suzuki, N.; Kamimura, J. Hydrogenolysis of diaryl and aryl alkyl ketones and carbinols by sodium borohydride and anhydrous aluminum(III) chloride. *Synthesis* **1987**, 736–738.
(31) Bieg, T.; Szeja, W. Removal of O-benzyl protective groups by catalytic transfer hydrogenation. *Synthesis* **1985**, 76–77.
(32) Li, X.; Hewgley, J. B.; Mulrooney, C. A.; Yang, J.; Kozlowski, M. C. Enantioselective oxidative biaryl coupling reactions catalyzed by 1,5-diazadecalin metal complexes: efficient formation of chiral functionalized BINOL derivatives. *J. Org. Chem.* **2003**, *68*, 5500–5511.
(33) Stoner, E. J.; Cothron, D. A.; Balmer, M. K.; Roden, B. A. Benzylation via tandem Grignard reaction−iodotrimethylsilane (TMSI) mediated reduction. *Tetrahedron* **1995**, *51*, 11043–11062.
(34) Cain, G. A.; Holler, E. R. Extended scope of in situ iodotrimethylsilane mediated selective reduction of benzylic alcohols. *Chem. Commun.* **2001**, 1168–1169.
(35) (a) Nakamura, H.; Wu, C.; Inouye, S.; Murai, A. Design, synthesis, and evaluation of the transition-state inhibitors of coelenterazine bioluminescence: probing the chiral environment of active site. *J. Am. Chem. Soc.* **2001**, *123*, 1523–1524. (b) Gribble, G. W.; Leese, R. M.; Evans, B. E. Reactions of sodium borohydride in acidic media. IV. Reduction of diarylmethanols and triarylmethanols in trifluoroacetic acid. *Synthesis* **1977**, 172–176.
(36) (a) Denner, K.; Bernhardt, R. Inhibition studies of steroid conversions mediated by human CYP11B1 and CYP11B2 expressed in cell cultures. In *Oxygen Homeostasis and Its Dynamics*, 1st ed.; Ishimura, Y., Shimada, H., Suematsu, M., Eds.; Springer-Verlag: New York, 1998; pp 231−236. (b) Denner, K.; Doehmer, J.; Bernhardt, R. Cloning of CYP11B1 and CYP11B2 from normal human adrenal and their functional expression in COS-7 and V79 chinese hamster cells. *Endocr. Res.* **1995**, *21*, 443–448. (c) Böttner, B.; Denner, K.; Bernhardt, R. Conferring aldosterone synthesis to human CYP11B1 by replacing key amino acid residues with CYP11B2-specific ones. *Eur. J. Biochem.* **1998**, *252*, 458–466.
(37) Lamberts, S. W.; Bruining, H. A.; Marzouk, H.; Zuiderwijk, J.; Uitterlinden, P.; Blijd, J. J.; Hackeng, W. H.; de Jong, F. H. The new aromatase inhibitor CGS-16949A suppresses aldosterone and cortisol production by human adrenal cells in vitro. *J. Clin. Endocrinol. Metab.* **1989**, *69*, 896–901.
(38) Demers, L. M.; Melby, J. C.; Wilson, T. E.; Lipton, A.; Harvey, H. A.; Santen, R. J. The effects of CGS 16949A, an aromatase inhibitor on adrenal mineralocorticoid biosynthesis. *J. Clin. Endocrinol. Metab.* **1990**, *70*, 1162–1166.
(39) Heim, R.; Lucas, S.; Grombein, C. M.; Ries, C.; Schewe, K. E.; Negri, M.; Müller-Vieira, U.; Birk, B.; Hartmann, R. W. Overcoming undesirable CYP1A2 inhibition of pyridylnaphthalene type aldosterone synthase inhibitors: Influence of heteroaryl derivatization on potency and selectivity. *J. Med. Chem.* **2008**, *15*, 5064−5074.
(40) (a) Ehmer, P. B.; Jose, J.; Hartmann, R. W. Development of a simple and rapid assay for the evaluation of inhibitors of human 17α-hydroxylase-C17,20-lyase (P450c17) by coexpression of P450c17 with NADPH-cytochrome-P450-reductase in *Escherichia coli*. *J. Steroid Biochem. Mol. Biol.* **2000**, *75*, 57–63. (b) Hutschenreuter, T. U.; Ehmer, P. B.; Hartmann, R. W. Synthesis of hydroxy derivatives of highly potent nonsteroidal CYP17 inhibitors as potential metabolites and evaluation of their activity by a noncellular assay using recombinant enzyme. *J. Enzyme Inhib. Med. Chem.* **2004**, *19*, 17–32.
(41) Thompson, E. A.; Siiteri, P. K. Utilization of oxygen and reduced nicotinamide adenine dinucleotide phosphate by human placental microsomes during aromatization of androstenedione. *J. Biol. Chem.* **1974**, *249*, 5364–5372.
(42) Hartmann, R. W.; Batzl, C. Aromatase inhibitors. Synthesis and evaluation of mammary tumor inhibiting activity of 3-alkylated 3-(4-aminophenyl)piperidine-2,6-diones. *J. Med. Chem.* **1986**, *29*, 1362–1369.
(43) Williams, P. A.; Cosme, J.; Ward, A.; Angove, H. C.; Matak Vinkovic, D.; Jhoti, H. Crystal structure of human cytochrome P4502C9 with bound warfarin. *Nature* **2003**, *424*, 464–468.
(44) Hindle, S. A.; Rarey, M.; Buning, C.; Lengauer, T. Flexible docking under pharmacophore type constraints. *J. Comput.-Aided Mol. Des.* **2002**, *16*, 129–149.
(45) Rarey, M.; Kramer, B.; Lengauer, T.; Klebe, G. A fast flexible docking method using an incremental construction algorithm. *J. Mol. Biol.* **1996**, *261*, 470–489.
(46) Rarey, M.; Kramer, B.; Lengauer, T. Multiple automatic base selection: protein−ligand docking based on incremental construction without manual intervention. *J. Comput.-Aided Mol. Des.* **1997**, *11*, 369–384.

JM800683C